ORNL/TM-6136

Criticality Considerations for ^{233}U Fuels in an HTGR Fuel Refabrication Facility

S. R. McNeany
J. D. Jenkins

OAK RIDGE NATIONAL LABORATORY
OPERATED BY UNION CARBIDE CORPORATION · FOR THE DEPARTMENT OF ENERGY

DISCLAIMER

Printed in the United States of America. Available from
National Technical Information Service
U.S. Department of Commerce
5285 Port Royal Road, Springfield, Virginia 22161
Price: Printed Copy $5.25; Microfiche $3.00

ORNL/TM-6136
Dist. Category UC-77

Contract No. W-7405-eng-26

Engineering Technology Division

CRITICALITY CONSIDERATIONS FOR ^{233}U FUELS IN AN HTGR FUEL REFABRICATION FACILITY

S. R. McNeany J. D. Jenkins

Date Published - January 1978

NOTICE: This document contains information of a preliminary nature. It is subject to revision or correction and therefore does not represent a final report.

Prepared by the
OAK RIDGE NATIONAL LABORATORY
Oak Ridge, Tennessee 37830
operated by
UNION CARBIDE CORPORATION
for the
DEPARTMENT OF ENERGY

THIS PAGE

WAS INTENTIONALLY

LEFT BLANK

CONTENTS

CRITICALITY CONSIDERATIONS FOR ^{233}U FUELS IN AN HTGR FUEL REFABRICATION FACILITY

S. R. McNeany J. D. Jenkins

ABSTRACT

Eleven ^{233}U solution critical assemblies spanning an $H/^{233}U$ ratio range of 40 to 2000 and a bare metal ^{233}U assembly have been calculated with the ENDF/B-IV and Hansen-Roach cross sections. The results from these calculations are compared with the experimental results and with each other. We observed an increasing disagreement between calculations with ENDF/B and Hansen-Roach data with decreasing $H/^{233}U$ ratio, indicative of large differences in their intermediate energy cross sections. The Hansen-Roach cross sections appeared to give reasonably good agreement with experiments over the whole range; whereas the ENDF/B calculations yielded high values for k_{eff} on assemblies of low moderation.

We conclude that serious problems exist in the ENDF/B-IV representation of the ^{233}U cross sections in the intermediate energy range and that further evaluation of this nuclide is warranted. In addition, we recommend that an experimental program be undertaken to obtain ^{233}U criticality data at low $H/^{233}U$ ratios for verification of generalized criticality safety guidelines.

In Part II of this report we present the results of criticality calculations on specific pieces of equipment required for HTGR fuel refabrication. In particular, we find that fuel particle storage hoppers and resin carbonization furnaces are criticality safe up to 22.9 cm (9.0 in.) in diameter providing water or other hydrogenous moderators are excluded. In addition we find no criticality problems arising due to accumulation of particles in the off-gas scrubber reservoirs provided reasonable administrative controls are exercised.

INTRODUCTION

Uranium-233 is a fissile isotope that will be generated in High-Temperature Gas-Cooled Reactors (HTGRs) and other nuclear power reactors operating on the thorium fuel cycle. To implement recycle of this uranium, facilities must be designed to chemically reprocess spent fuel and refabricate the ^{233}U into fuel elements. Criticality safety is an important concern that must be incorporated into the design of fuel recycle equipment containing ^{233}U.

The American National Standards Institute has formulated generalized guidelines[1] for safe operations with fissile materials outside reactors. For homogeneous aqueous solutions and slurries of ^{233}U, the limits are given in terms of fissile mass, geometric dimensions and concentration of the fissile nuclide. The limit on any one of the above parameters is set to prevent accidental criticality for all practical* combinations of other parameters.

Often, the published limits impose impractical restraints on process equipment. The standard acknowledges this and includes provisions for control by neutron absorbers and administrative procedures. In those cases where generalized subcritical limits must be exceeded to allow for less stringent restraints on material containers, the standard specifies that subcritical limits should be established on the basis of data obtained from experiments. When applicable experimental data do not exist, the limits may be set by calculations that have been shown to be valid by comparison with experimental data.

If calculations are to be used to set subcritical conditions, precise experimental criticality data are desirable to validate calculational techniques and neutron cross sections before the calculations can be confidently extended to criticality problems found in fuel processing equipment. For cross section validation, experimental criticality data should be supplied for simple geometry systems (spheres or right cylinders are usually used) to simplify validation calculations.

Caution must be exercised in extending calculations to systems with neutron energy spectra outside the range of those in the critical experiments used for validation. As neutron energy spectra change, reactivity dependence can shift to energy regions where cross sections have not been validated. Since fuel processing facilities can contain material in many forms, from highly moderated to material containing little or no moderation, benchmark critical experiments are needed over a wide range of neutron energy spectra for validation of calculations.

---

*It is assumed that highly effective neutron reflectors such as beryllium and D_2O will not be present.

PART I. EVALUATION OF ^{233}U CROSS SECTIONS FOR CRITICALITY SAFETY ANALYSIS

THIS PAGE

WAS INTENTIONALLY

LEFT BLANK

1. CURRENT STATUS OF ^{233}U CRITICAL EXPERIMENTS IN SIMPLE GEOMETRY

Very little experimental criticality data are currently available on ^{233}U systems compared to that available on ^{235}U systems. The shortage of data is especially acute for ^{233}U systems having low moderation (i.e., $\sim 1 < H/^{233}U < \sim 40$). There are at least three reasons for this lack of data. First, ^{233}U is always accompanied by trace amounts of ^{232}U which has highly radioactive daughter nuclides that make handling difficult; second, ^{233}U with low parts per million ^{232}U has been reserved mainly for the military; and third, past demands for such data have been overshadowed by those for ^{235}U systems. A search of the literature[2-8] yields the sets of experiments listed in Table 1 as those available for validation of criticality calculations. The lack of data on low moderation systems is quite apparent. In addition, examination of Ref. 3 reveals that experimental difficulties were encountered on some of the lowest moderation systems.

The full impact of the lack of data on low moderation systems is best appreciated when viewed in the light of the work of J. W. Webster.[9] In his investigations Webster shows that the most reactive ^{233}U solutions have $H/^{233}U$ ratios of about 40 for cylinders and spheres and 25 for slabs. These solution concentrations fall in the region where critical experiments are lacking. Hence, very little data are available to verify the maximum dimensional limits for ^{233}U criticality control as published in the standards.

The personnel of the HTGR Fuel Recycle Program at Oak Ridge National Laboratory (ORNL) recognized the need for additional ^{233}U criticality data and issued a subcontract under the Thorium Utilization Program to Battelle Pacific Northwest Laboratories (BPNL) to prepare a detailed plan for performance of ^{233}U critical experiments. The experiment plan has been completed and issued as a BNWL report.[10] Unfortunately, due to cutbacks in the funding of the Thorium Utilization Program, the experiments have not yet been performed. No other plans for ^{233}U experiments are known to the authors at present.

Table 1. Summary of ^{233}U critical experiments

Experiments	$H/^{233}U$ ratios	Reference
Spheres of uranium metal with and without reflectors of natural uranium, beryllium, and tungsten alloy	0	2
Spheres and cylinders of aqueous solutions of UO_2F_2 and $UO_2(NO_3)_2$ with and without reflectors of water and paraffin	34.2—775	3
Spheres and cylinders of aqueous solutions of $UO_2(NO_3)_2$ with and without water reflectors	73—581	4
Cylinders of aqueous solutions of $UO_2(NO_3)_2$ with and without reflectors	120—1050	5
Spheres of aqueous solutions of UO_2F_2 with water reflectors at temperatures from 26°C to 100°C	378—663	6
Large unreflected spheres and cylinders of aqueous solutions of $UO_2(NO_3)_2$ with and without neutron poisons	1324—2106	7
Unreflected sphere of aqueous solution of $UO_2(NO_3)_2$	1521	8

2. DISCREPANCIES OBSERVED IN ^{233}U CRITICALITY CALCULATIONS

In April 1973, a report[11] was issued at Oak Ridge on ^{233}U criticality calculations performed in support of the HTGR fuel refabrication process. These were to be used as guidelines in criticality control. The calculations involved simple geometries and used the Hansen-Roach[12] cross-section set. Several of the same cases were analyzed by BPNL[13] using ENDF/B-III[14] derived cross sections. The Battelle work indicated large differences in computed critical masses between the ENDF and Hansen-Roach results. In particular, differences in critical mass ranged between 14% and 56% for cases of water-reflected homogeneous spheres of ^{233}U and ^{233}U—^{232}Th mixtures. Table 2, which is taken directly from the Battelle report, compares their calculations with those of the Oak Ridge report.

Discrepancies of this magnitude are extremely distressing to designers of ^{233}U fuel handling equipment. On the one hand, designers would like fuel containing vessels to be large so that high throughput can be obtained from individual pieces of equipment while on the other, criticality safety must be maintained at all costs. If neither cross-section set can be validated by comparison with accurate experimental data, over-conservative size limitations may have to be imposed upon costly fuel processing equipment.

To investigate Battelle's reported calculational discrepancies between ENDF/B and Hansen-Roach cross sections and to attempt to verify one of the two sets, a more extensive criticality study was undertaken. The method of calculation and the results of the study are presented below.

Table 2. Comparison between calculated critical conditions for homogeneous fuel mixtures typical of the HTGR fuel cycle[a]

$H/^{233}U$ (atom ratio)	$C/^{233}U$ (atom ratio)	^{233}U (g/cm^3)	Water-reflected spheres			
			ENDF/B + DTF-IV[b]		Hansen-Roach + ANISN[c]	
			Critical radius (cm)	Critical mass (kg ^{233}U)	Critical radius (cm)	Critical mass (kg ^{233}U)
			← 0 $^{232}Th/^{233}U$ →			
2	0	5.433	7.64	10.15	8.25	12.77
2	100	0.328	26.17	24.62	29.5	35.27
500	100	0.045	14.44	0.57	15.1	0.65
			← 4 $^{232}Th/^{233}U$ →			
2	0	1.568[d]	17.02	32.38	18.95	46.61
2	122.1	0.242[d]	36.82	50.60	42.55	78.73
500	122.1	0.043	16.02	0.74	16.81	0.85

[a] Ref. 13.

[b] Calculated values using ENDF/B data processed by ETOG and FLANGE and averaged over 18 energy groups by EGGNIT for use in DTF-IV.

[c] Calculated values reported by Thomas, Ref. 11.

[d] Higher densities reported in Ref. 11 as a result of using an oxide density of 10.65 g/cm^3 instead of a mixture density based on 10.65 g UO_2/cm^3 and 10.03 ThO_2/cm^3.

3. CALCULATIONAL PROCEDURE

Two cross-section sets were used in this study. The first is the ENDF/B-IV library which is available from Brookhaven National Laboratory (BNL), and the second is a 16-group Hansen-Roach library used at ORNL. Both of these libraries have been described in the literature.[12,14]

To utilize the ENDF data for criticality calculations, a 123-energy-group P_3 "master library" was generated. This library consisted of flux-averaged smooth cross sections plus resonance parameters. The assumed flux shape used in the fine-group averaging procedure was a Maxwellian (at 300°K) from zero to 0.1265 eV connected to a 1/E spectrum to 67.4 keV. Above this energy a Maxwellian fission spectrum with an effective "temperature" of 1.273 MeV was assumed. XLACS, a processing code which is part of the AMPX code package,[15] was used to generate the master library. NITAWL, also part of the AMPX package, was then used to form problem-dependent, resonance self-shielded cross sections from the master library. The Nordheim integral treatment[16] was used for these calculations.

The second cross-section set used in this investigation is the 16-group Hansen-Roach set. Some of the nuclides in this library contain P_o and P_1 scattering matrices. Others have only a P_o representation. No resonance parameters are given. Resonance self-shielding is accounted for by the inclusion of multiple cross-section sets for resonance nuclides (i.e., those nuclides where resonance self-shielding may play an important role). The selection of a particular set for a resonance nuclide is made on the basis of a problem dependent, potential scattering cross section per resonance nuclide atom (σ_p) in the medium containing the resonance nuclide.

With the problem-dependent cross sections in hand, XSDRNPM,[15] ANISN[17] (one-dimensional discrete ordinates codes) or KENO-IV[18] (a Monte Carlo code), were used to solve the neutron transport equation. An S_8 quadrature was used for all the discrete ordinates calculations.

4. CONFIRMATION OF BATTELLE'S REPORTED CALCULATION DISCREPANCIES

To confirm the discrepancies between calculations performed with Hansen-Roach and ENDF/B cross sections reported by Battelle, the first three cases in Table 2 were recalculated with the Hansen-Roach library and our 123-group ENDF/B library. Descriptions of the composition, geometry and calculated critical radii of these cases are given in Tables 3 and 4. As expected, the results of our calculations using Hansen-Roach cross sections were identical to those of the earlier Oak Ridge report. For the cases using ENDF/B cross sections, the critical radius was calculated for comparison with the Battelle predictions. Table 5 presents the results of these calculations. Based on these results which agreed to better than 3% with Battelle, we were convinced that the discrepancies observed by Battelle were real and that additional study of the problem was warranted.

Table 3. Atomic number densities[a] of three water-reflected[b] theoretical ^{233}U systems

Material	System		
	1	2	3
^{233}U	1.404(−2)	8.477(−4)	1.160(−4)
H	2.808(−2)	1.695(−3)	5.802(−2)
O	4.212(−2)	2.543(−3)	2.924(−2)
C	0	8.477(−2)	1.160(−2)

[a] (10^{24} atoms/cm^3).

[b] Reflector composition: H, 6.666(−2); O, 3.333(−2).

Table 4. Geometry description of three theoretical ^{233}U systems

	System		
	1	2	3
Geometry	Sphere	Sphere	Sphere
ENDF/B-III[a] calculated critical radius, cm	7.64	26.17	14.44
Hansen-Roach[b] calculated critical radius, cm	8.25	29.5	15.1
Reflector thickness, cm	20.0	20.0	20.0

[a]Calculated values reported in Ref. 13.

[b]Calculated values reported in Ref. 11.

Table 5. ENDF/B-IV calculations of critical radius for three theoretical ^{233}U systems

Case No.	$H/^{233}U$ ratio	$C/^{233}U$ ratio	^{233}U (g/cm^3)	Critical radius[a] (cm)	Critical radius[b] (cm)
1	2	0	5.433	7.64	7.73 ($k=1.001\pm0.005$)[c]
2	2	100	0.328	26.17	25.40[d]
3	500	100	0.045	14.44	14.57[d]

[a]BPNL calculation.

[b]Present work.

[c]KENO Monte Carlo calculation.

[d]XSDRN S_n calculations.

5. CALCULATIONS OF SELECTED ^{233}U CRITICAL EXPERIMENTS

Having confirmed that serious discrepancies exist between results calculated with Hansen-Roach and ENDF/B cross sections, we undertook a comparison of both data sets with existing critical experiments. Twelve experiments were selected for calculation. These were picked to cover a wide range in $H/^{233}U$ ratios. Table 6 lists the selected experiments along with their $H/^{233}U$ ratio, the reported experimental uncertainty in critical mass, and our estimate of how this uncertainty translates to an equivalent uncertainty in k_{eff}.*

Tables listing the atomic number densities and geometry descriptions for the twelve experiments are given in Tables 7 and 8. Using these descriptions, k_{eff} was calculated for each assembly. Table 9 and Fig. 1 give the results. The errors indicated in Table 9 and the error bars shown on the figure represent one standard deviation (68% confidence interval about the mean value) as calculated by KENO, a Monte Carlo code. To check agreement between KENO and XSDRNPM, a discrete ordinates code, two of the experiments were calculated by both codes. In both cases, the XSDRNPM result fell within two standard deviations (95% confidence interval) of the KENO result.

The calculated results differ significantly from the experimental results for a number of the systems. In general, agreement between calculation and experiment is good on systems having high $H/^{233}U$ ratios; however, as lower $H/^{233}U$ ratios are approached significant deviations appear between calculated results and experimental results. Specifically, k_{eff} calculated with Hansen-Roach cross sections tends to be low in most cases while ENDF/B-IV results tend to be high. In the case of the metal sphere this situation is reversed. Overall, the differences between calculated results and experimental results using ENDF/B-IV data are larger than those obtained using the Hansen-Roach cross-section set. Two exceptions are experiments 5 and 7. Here the ENDF/B results are quite

---

*The uncertainty in k_{eff} from an exact calculation of a system with a reported critical mass, m_c, and an uncertainty dm_c, can be estimated from the relation $dK/K \sim dm_c/m_c$ (1-f), where f is the thermal utilization for the system.[19]

Table 6. List of ^{233}U critical experiments selected for calculation

Experiment number	Description	Reference	$H/^{233}U$ ratio	Reported experimental uncertainties	Uncertainty range of calculated k_{eff}
1	Unreflected sphere of U metal	2	0.0	m_c[a] uncertain by ±0.3%	0.9992 – 1.0008
2	Fully reflected cylinder of aqueous UO_2F_2 solution	3	39.4	m_c too high by an amount not well known but probably less than 10%	1.0000 – 1.0025
3	Fully reflected cylinder of aqueous UO_2F_2 solution	3	45.9	m_c too high by an amount not well known but probably less than 10%	1.0000 – 1.0028
4	Unreflected cylinder of aqueous $UO_2(NO_3)_2$ solution	4	73.0	m_c uncertain by ±0.5%	0.9997 – 1.0003
5	Partially reflected cylinder of aqueous UO_2F_2 solution	3	74.1	m_c too high by about 2% and uncertain by ±0.5%	1.0007 – 1.0013
6	Fully reflected cylinder of aqueous $UO_2(NO_3)_2$ solution	3	84.4	m_c uncertain by ±2.5%	0.9986 – 1.0014
7	Unreflected cylinder of aqueous $UO_2(NO_3)_2$ solution	4[b]	119	m_c uncertain by ±0.5%	0.9996 – 1.0004
8	Unreflected cylinder of aqueous UO_2F_2 solution	3	154	m_c uncertain by ±2.5%	0.9973 – 1.0027
9	Unreflected sphere of aqueous $UO_2(NO_3)_2$ solution	4	195	m_c uncertain by ±0.5%	0.9994 – 1.0006
10	Unreflected sphere of aqueous UO_2F_2 solution	3	381	m_c too high by about 2% and uncertain by ±1%	1.0018 – 1.0054
11	Unreflected sphere of aqueous $UO_2(NO_3)_2$ solution	7	1533	m_c uncertain by ±0.5%	0.9976 – 1.0024
12	Unreflected sphere of aqueous $UO_2(NO_3)_2$ solution	7	1986	m_c uncertain by ±0.5%	0.9973 – 1.0027

[a] Critical mass.

[b] This experiment is also described in Ref. 19.

Table 7. Atomic number densities[a] of selected highly enriched ^{233}U critical experiments

Material	Experiment											
	1	2[b]	3[b]	4	5[b]	6	7	8	9	10	11	12
^{233}U	4.670(-2)	1.551(-3)	1.341(-3)	8.394(-4)	8.575(-4)	7.107(-4)	5.141(-4)	4.264(-4)	3.302(-4)	1.735(-4)	4.328(-5)	3.346(-5)
^{234}U	5.925(-4)	8.448(-6)	7.307(-6)	8.997(-6)	8.671(-6)	3.585(-6)	5.518(-6)	2.323(-6)	3.540(-6)	9.452(-7)	7.160(-7)	5.250(-7)
^{235}U	1.416(-5)	6.232(-7)	5.389(-7)	2.560(-7)	2.445(-7)	7.139(-8)	1.370(-7)	1.713(-7)	1.007(-7)	6.972(-8)	1.800(-8)	1.000(-8)
^{238}U	2.843(-4)	1.107(-5)	9.578(-6)	1.171(-5)	8.124(-6)	5.569(-6)	7.305(-6)	3.045(-6)	4.607(-6)	1.239(-6)	2.310(-7)	2.560(-7)
^{232}Th		0	0	0	0	0	0	0	0	0	1.964(-7)	1.476(-7)
N	0	0	0	1.721(-3)	0	1.890(-3)	1.295(-3)	0	6.769(-4)	0	1.178(-4)	7.530(-5)
H	0	6.111(-2)	6.156(-2)	6.128(-2)	6.354(-2)	5.998(-2)	6.137(-2)	6.567(-2)	6.439(-2)	6.611(-2)	6.636(-2)	6.647(-2)
O	0	3.370(-2)	3.350(-2)	3.752(-2)	3.351(-2)	3.688(-2)	3.550(-2)	3.370(-2)	3.490(-2)	3.341(-2)	3.361(-2)	3.353(-2)
F	0	3.141(-3)	2.717(-3)	0	2.737(-3)	0	0	8.639(-4)	6.769(-4)	3.515(-4)	0	0
$H/^{233}U$	0.0	39.4	45.9	73.0	74.1	84.4	119.4	154.0	195.0	381.0	1533	0

[a] (10^{24} atoms/cm^3).

[b] Reflector composition: H, 7.734(-2); C, 3.867(-2).

Table 8. Geometry description of selected highly enriched ^{233}U critical experiments

	Experiment											
	1	2	3	4	5	6	7	8	9	10	11	12
Geometry	Sphere	Cylinder	Cylinder	Cylinder	Cylinder	Cylinder	Cylinder	Cylinder	Sphere	Sphere	Sphere	Sphere
Critical radius (cm)	5.984	8.35	8.35	25.40	7.55	10.25	12.70	12.75	14.58	15.94	34.59	61.01
Critical height (cm)	—	16.7 ± 0.2[a]	16.9	13.36	24.0	14.7	24.69	24.00	—	—	—	—
Reflector thickness (cm)	None	20.0	20.0	None	20.0[b]	20.0	None	None	None	None	None	None

[a] Extrapolated value derived from source neutron multiplication curve. Maximum subcritical height was 16.3 cm.

[b] No reflector on top surface.

Table 9. Results of Hansen-Roach and ENDF/B-IV cross section calculations on highly enriched ^{233}U critical experiments

Experiment number	Description	$H/^{233}U$ ratio	Expected range of values for calculated k_{eff}	Calculated k_{eff}[a]	
				Hansen-Roach	ENDF/B-IV
1	Unreflected sphere of uranium metal	0.0	0.9992–1.0008	1.008 (ANISN)[b]	0.967 (XSDRNPM)
2	Fully reflected cylinder of aqueous UO_2F_2 solution	39.4	1.0000–1.0025	1.006 ± 0.007 (KENO)	1.066 ± 0.006 (KENO)
3	Fully reflected cylinder of aqueous UO_2F_2 solution	45.9	1.0000–1.0028	1.003 ± 0.006 (KENO)	1.054 ± 0.006 (KENO)
4	Unreflected cylinder of aqueous $UO_2(NO_3)_2$ solution	73.0	0.9997–1.0003	0.995 ± 0.007 (KENO)	1.041 ± 0.006 (KENO)
5	Partially reflected cylinder of aqueous UO_2F_2 solution	74.1	1.0007–1.0013	0.983 ± 0.006 (KENO)	1.012 ± 0.007 (KENO)
6	Fully reflected cylinder of aqueous $UO_2(NO_3)_2$ solution	84.4	0.9986–1.0014	1.002 ± 0.006 (KENO)	1.044 ± 0.006 (KENO)
7	Unreflected cylinder of aqueous $UO_2(NO_3)_2$ solution	119	0.9996–1.0004	0.958 ± 0.007 (KENO)	1.003 ± 0.007 (KENO)
8	Unreflected cylinder of aqueous UO_2F_2 solution	154	0.9973–1.0027	0.990 ± 0.006 (KENO)	1.022 ± 0.007 (KENO)
9	Unreflected sphere of aqueous $UO_2(NO_3)_2$ solution	195	0.9994–1.0006	0.944 (ANISN)	1.028 (XSDRNPM)
10	Unreflected sphere of aqueous UO_2F_2 solution	381	1.0018–1.0054	0.988 (ANISN)	1.013 (XSDRNPM) 1.007 ± 0.006 (KENO)
11	Unreflected sphere of aqueous $UO_2(NO_3)_2$ solution	1533	0.9976–1.0024	1.004 (ANISN)	0.996 (XSDRNPM) 0.998 ± 0.004 (KENO)
12	Unreflected sphere of aqueous $UO_2(NO_3)_2$ solution	1986	0.9973–1.0027	1.005 (ANISN)	0.991 (XSDRNPM)

[a] Errors represent one standard deviation on calculated mean value (i.e., 68% confidence interval).

[b] Names in parentheses indicate codes used to calculate k_{eff}.

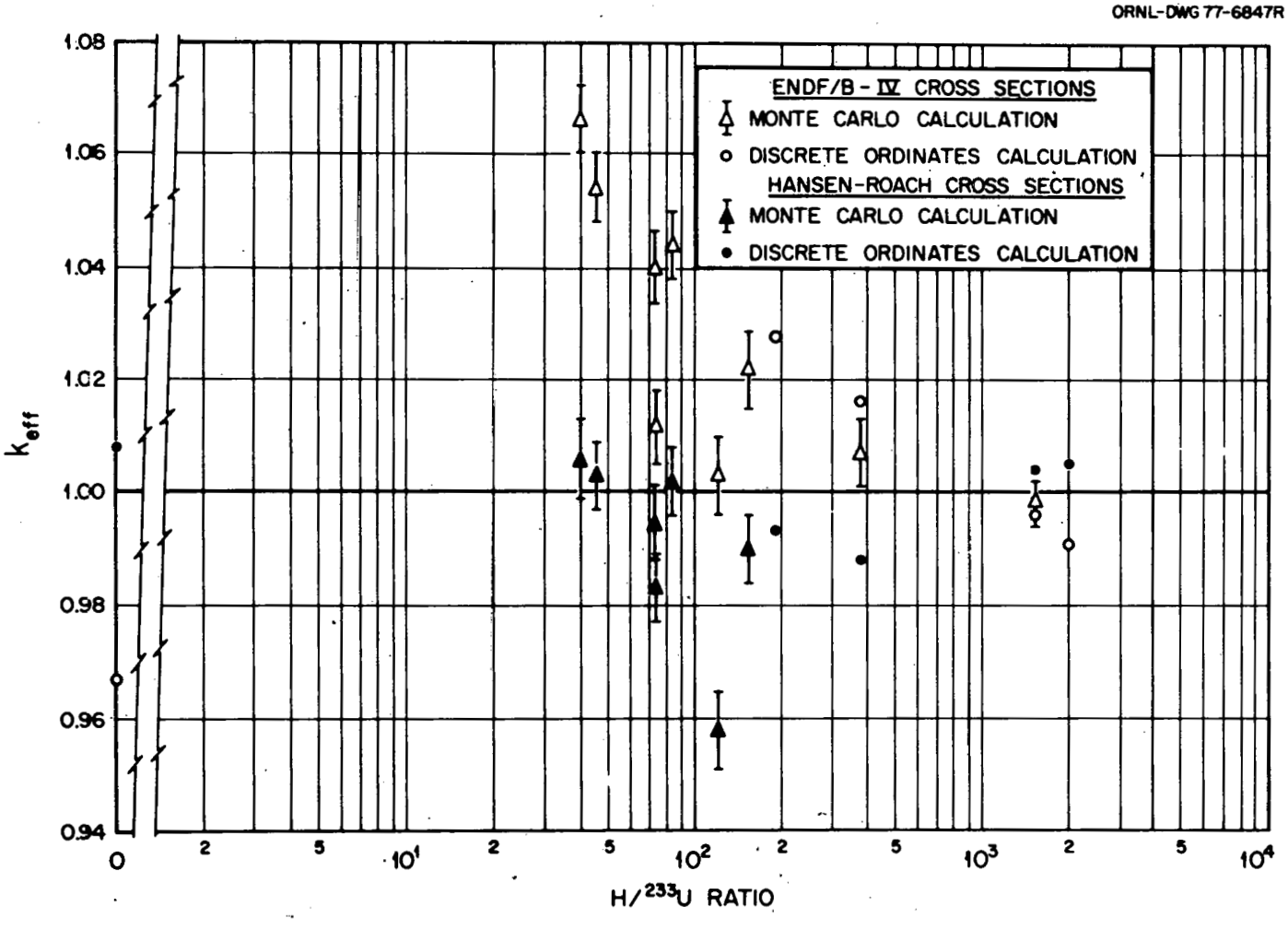

Fig. 1. Comparison between ENDF/B-IV and Hansen-Roach cross section calculations of experimental ^{233}U critical assemblies.

good. In particular, experiment 7 having the highest degree of experimental accuracy, agrees very well with the ENDF/B prediction.

To further pursue the differences between calculations with the two cross-section sets, we examined the ratio of k_{eff} calculated with ENDF/B-IV cross sections to k_{eff} calculated with Hansen-Roach data. Henceforth, we will refer to this ratio as the k_{eff} ratio. Figure 2 displays the k_{eff} ratio as a function of $H/^{233}U$ for each of the twelve experiments and for eight theoretical systems described in Tables 10 and 11. Seven of the theoretical systems are unreflected spheres of $^{233}UO_2$ powder and polyethylene homogeneously mixed to give $H/^{233}U$ ratios identical to those of experiments 2, 3, 5, 6, 7, 8 and 11. They were constructed to allow calculation with one-dimensional S_n theory and thus remove the statistical uncertainties introduced by the Monte Carlo calculations of the corresponding critical experiments. In particular, we wanted to determine if the dip in the k_{eff} ratio at $H/^{233}U$ values of 70 to 90 was attributable to cross section effects or to statistical and geometric uncertainties. The smooth increase in the k_{eff} ratio over the whole $H/^{233}U$ range predicted by our theoretical systems confirmed our expectation that the inflection in the ratio observed for the critical experiment calculations was not due to the ^{233}U cross sections, but probably to statistical uncertainties introduced by the Monte Carlo calculations.

As seen in Fig. 2, the k_{eff} ratio for the theoretical systems increases smoothly with decreasing moderation over the experimental range of $H/^{233}U$ ratio from 2000 to 40. To project this trend, a calculation was performed on the eighth theoretical system having an $H/^{233}U$ of 5. A k_{eff} ratio of 1.12 was obtained for this system. Corresponding to this k_{eff} ratio there exists a difference in calculated critical mass of 40% — a rather large and disturbing result.

The trend of increasing differences between calculations with the two cross-section sets with decreasing moderation is related to a changing neutron energy spectrum. The shape of the neutron energy spectrum for a given system determines which energy regions (and cross-section groups) contribute most to the calculated result. For example, in the ^{233}U metal sphere with an $H/^{233}U$ ratio of zero, the high energy groups are the main contributors to the system multiplication. Less than 10^{-8}% of the total

Table 10. Atomic number densities[a] of eight theoretical ^{233}U systems

Material	System							
	1	2	3	4	5	6	7	8
^{233}U	9.537(-3)	1.181(-3)	1.577(-3)	1.001(-3)	8.832(-4)	6.329(-4)	4.919(-4)	5.031(-5)
H	4.769(-2)	7.164(-2)	7.239(-2)	7.418(-2)	7.454(-2)	7.532(-2)	7.576(-2)	7.713(-2)
C	2.384(-2)	3.582(-2)	3.619(-2)	3.709(-2)	3.727(-2)	3.766(-2)	3.788(-2)	3.856(-2)
O	1.908(-2)	3.637(-3)	3.154(-3)	2.002(-3)	1.766(-3)	1.266(-3)	9.838(-4)	1.006(-4)
H/U	5	39.4	45.9	74.1	84.4	119.4	154.0	1533

[a] (10^{24} atoms/cm^3).

Table 11. Geometry description of eight theoretical ^{233}U systems

	System							
	1	2	3	4	5	6	7	8
Geometry	Sphere	Sphere	Sphere	Sphere	Sphere	Sphere	Sphere	Sphere
Hansen-Roach calculated critical radius (cm)	11.180	11.419	11.445	11.602	11.671	11.911	12.166	29.126
Reflector thickness (cm)	None	None	None	None	None	None	None	None

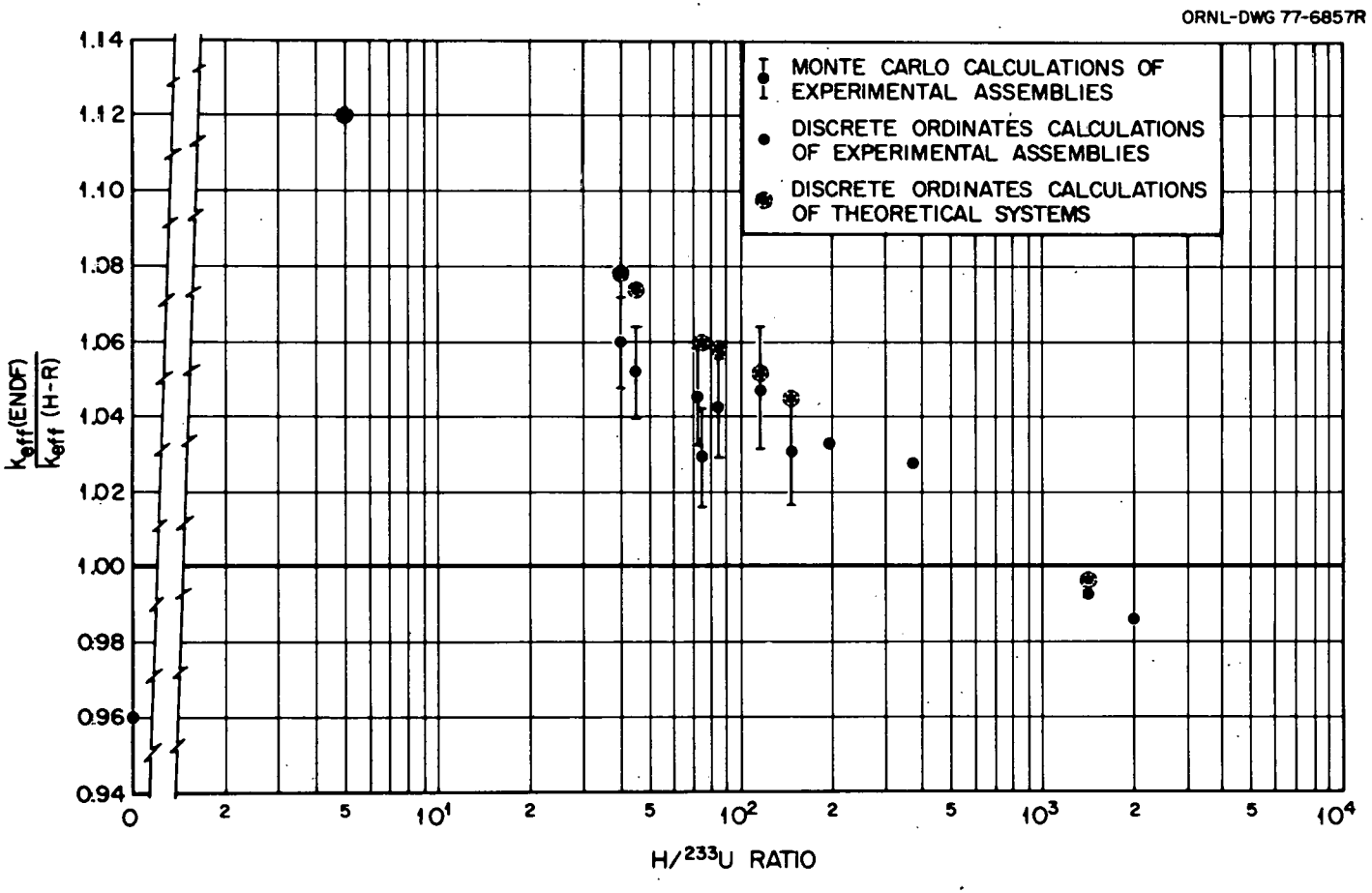

Fig. 2. Ratios of effective neutron multiplication constants calculated by ENDF/B-IV and Hansen-Roach cross sections for experimental and theoretical critical assemblies of ^{233}U.

number of fissions take place in the energy range below 1.86 eV. Thermal cross sections are not important in this problem. On the other hand, a problem having an $H/^{233}U$ ratio of 1533 has more than 96% of the fissions taking place in the energy range below 1.86 eV. Here, the thermal cross sections are very important.

Figure 3 shows a plot of the calculated fission rate per unit lethargy as a function of energy for three of the critical experiments. Experiment 1, a ^{233}U metal sphere, displays a characteristic fast spectrum, while experiment 11, having an $H/^{233}U$ ratio of 1533, represents a well-thermalized system. Experiment 2, with a core $H/^{233}U$ ratio of 39.4, has a substantial epithermal component. This plus the observed increasing deviation between ENDF/B based calculations and experiment as the H/U ratio is reduced (see Fig. 1) leads us to conclude that problems may exist in the ENDF/B ^{233}U epithermal representation.

In Fig. 3 note also the extreme change in the fission rate distribution between experiment 1 and experiment 2. This suggests that even if a cross-section set were validated for these two experiments, it would not necessarily give correct results for intermediate systems. Additional data would be required to validate calculations on very low $H/^{233}U$ ratio systems.

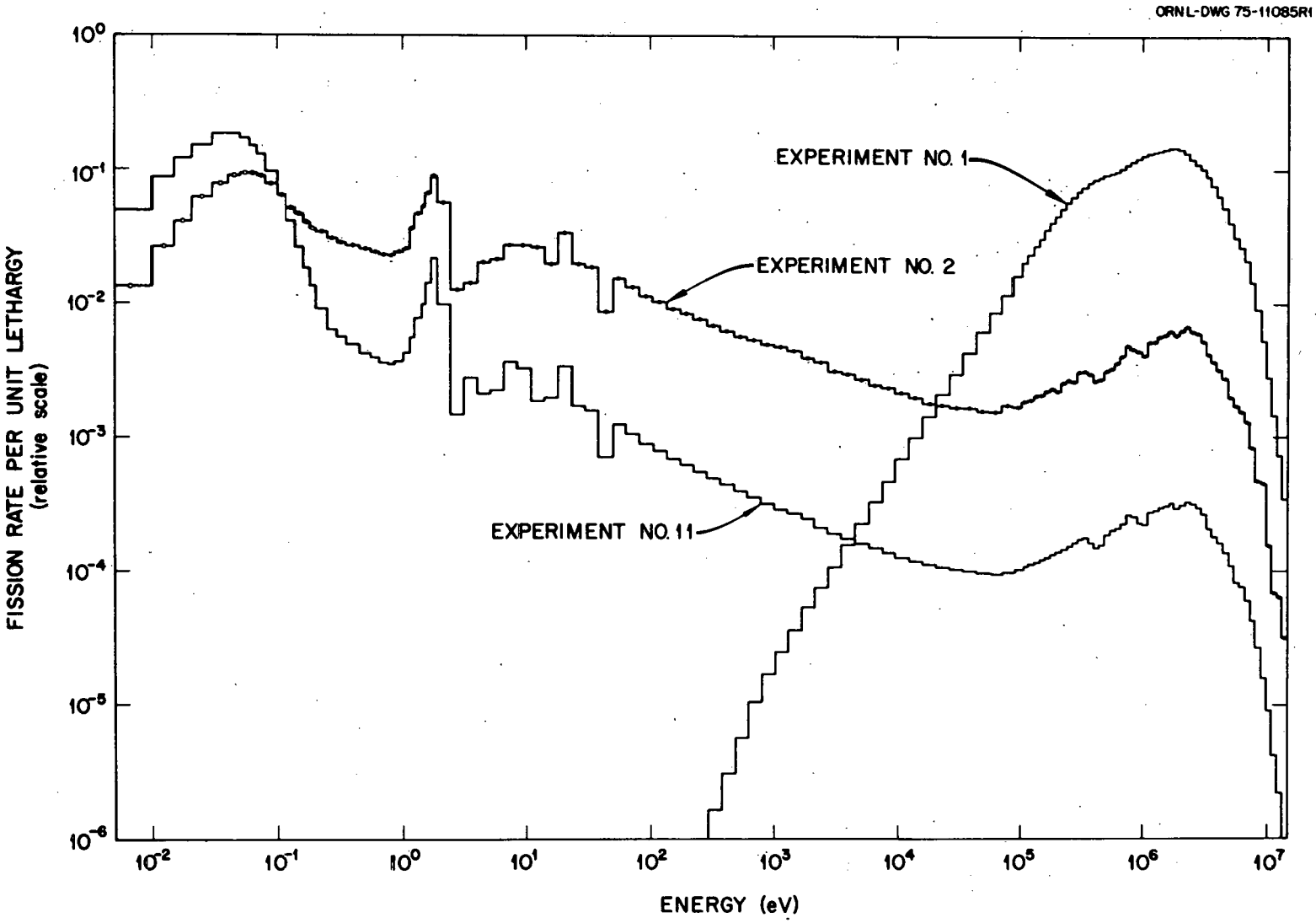

Fig. 3. Energy-dependent fission rate for three ^{233}U critical experiments.

6. CALCULATIONS OF SELECTED ^{235}U CRITICAL EXPERIMENTS

To verify the accuracy of our computational techniques k_{eff} was calculated for three critical experiments using highly enriched ^{235}U and having $H/^{235}U$ ratios of 0, 50.1 and 1393. A theoretical system with an $H/^{235}U$ ratio of 5.0 was also calculated. The calculations were done using the ENDF/B-IV and Hansen-Roach cross sections.

The three experiments chosen for analysis are described in Table 12. A complete description of the atomic compositions and geometry is given in Tables 13 and 14. The results are given in Table 15. Good agreement was obtained between these calculations and the experimental measurements. These results tend to confirm the cross-section processing procedure for ENDF/B-IV and Hansen-Roach cross sections and the neutron transport calculations.

Calculations of the theoretical ^{235}U system resulted in a k_{eff} ratio of 1.014. Thus, no large difference appears between ENDF/B-IV and Hansen-Roach cross-section calculations for ^{235}U systems.

Table 12. List of ^{235}U critical experiments selected for calculation

Experiment number	Description	Reference	$H/^{235}U$ ratio	Reported experimental uncertainties	Uncertainty range of calculated k_{eff}
13	Unreflected sphere of uranium metal	2	0.0	m_c uncertain by ±0.3%	0.9992–1.0008
14	Unreflected cylinder of aqueous UO_2F_2 solution	20	50.1	None reported assume m_c uncertain by ±0.5%	0.9999–1.0001
15	Unreflected sphere of aqueous UO_2F_2 solution	8	1393	m_c uncertain by ±1.0%	0.9969–1.0040

Table 13. Atomic number densities[a] of highly enriched ^{235}U critical experiments

Material	Experiment		
	13	14	15
^{234}U	0	0	5.864(-7)
^{235}U	4.500(-2)	1.230(-3)	4.774(-5)
^{238}U	2.982(-3)	8.860(-5)	2.864(-6)
H	0	6.162(-2)	6.650(-2)
O	0	3.345(-2)	3.335(-2)
F	0	2.637(-3)	1.024(-4)

[a] (10^{24} atoms/cm^3).

Table 14. Geometry description of highly enriched ^{235}U critical experiments

	Experiment		
	13	14	15
Geometry	Sphere	Cylinder	Sphere
Critical radius (cm)	8.741	15.24	34.60
Critical height (cm)	—	22.6	—
Reflector thickness (cm)	None	None	None

Table 15. Results of Hansen-Roach and ENDF/B-IV cross section calculations on highly enriched ^{235}U critical experiments

Experiment number	Description	$H/^{235}U$ ratio	Expected range of values for calculated k_{eff}	Calculated k_{eff}[a]	
				Hansen-Roach	ENDF/B-IV
13	Unreflected sphere of uranium metal	0.0	0.9992–1.0008	0.997 (ANISN)[b]	1.005 (XSDRNPM)
14	Unreflected cylinder of aqueous UO_2F_2 solution	50.1	0.9999–1.0001	0.986 ± 0.006 (KENO)	1.009 ± 0.006 (KENC)
15	Unreflected sphere of aqueous UO_2F_2 solution	1393	0.9960–1.0040	1.009 (ANISN)	0.998 ± 0.003 (KENC)

[a] Errors represent one standard deviation on calculated mean value (i.e., 68% confidence interval).

[b] Names in parentheses indicate codes used to calculate k_{eff}.

7. CONCLUSIONS

Our evaluation of Hansen-Roach and ENDF/B-IV ^{233}U cross sections confirms the large calculational discrepancies reported by Battelle. The largest differences between the calculations occur on undermoderated systems. Specifically, a 12% difference in calculated k_{eff} is found for a system with an $H/^{233}U$ ratio of 5. This corresponds to a 40% difference in calculated critical mass. For systems with $H/^{233}U$ ratios in the range of 1500–2000, the two data sets agree to within ∿1% in calculated k_{eff}.

Comparison of the calculated and experimental results showed good agreement for both cross section sets on systems having $H/^{233}U$ ratios in the 1500–2000 range. However, with decreasing $H/^{233}U$ ratio, the ENDF/B-IV calculations tended to predict k_{eff}'s that were too high. The Hansen-Roach results agreed well with experiment for these undermoderated systems. For the metal sphere, the ENDF/B-IV result was low while again the Hansen-Roach result was about right. From this we conclude that there are problems with the ENDF/B-IV cross section representation of the ^{233}U cross sections and that additional cross section evaluation work is warranted in this area.

We also recommend that additional ^{233}U critical experiments be performed on low moderation systems (i.e., $5 < H/^{233}U < 40$) where the calculational problems appear to be the most severe. This data could also serve to validate dimensional limits set down in criticality safety guides since these are based on low moderation systems. Specifically we note that the *American National Standard for Nuclear Safety in Operations with Fissionable Materials Outside Reactors*[1] gives the safe diameter of cylindrical containers for ^{233}U solutions as 11.5 cm. This value is based on a Hansen-Roach calculated k_{eff} of 0.98 for a solution with an $H/^{233}U$ ratio of 40. Because of the uncertainties in the existing experimental data on low moderation systems, we believe that a larger degree of conservatism should be applied to the determination of a safe diameter until the cross sections can be absolutely verified by precise criticality experiments of low moderation.

PART II. ^{233}U CRITICALITY CALCULATIONS FOR HTGR FUEL REFABRICATION EQUIPMENT

THIS PAGE

WAS INTENTIONALLY

LEFT BLANK

1. INTRODUCTION

All nuclear fuel handling facilities must incorporate criticality safety as an integral part of their operations. Therefore, during the early phases of plant design, specific criticality safety criteria must be established for each component of the plant as well as for the plant as a whole.

In Part II of this report, we present a brief overview of the HTGR fuel refabrication process as currently envisioned and a criticality analysis of two specific problem areas that will have significant influence on the design of a refabrication facility.

2. HTGR FUEL REFABRICATION PROCESS

Figure 4 shows the basic process steps for refabrication HTGR fuel.[21] Fissile material will enter the system in the form of uranyl nitrate solution (125 g/liter) stripped of fission products. In the first operation, spherical fuel kernels, approximately 400 μm in diameter, are prepared by loading uranyl nitrate on ion exchange resin. This operation is followed by a carbonization step to form a UO_2-C particle.

The carbonized resin is then passed to the Microsphere Conversion and Coating step where, in sequential operations in the same furnace, the material is converted to $UC_2 + UO_2$ and four layers of coating are deposited on the individual fuel kernels. The coatings, from inside out, are: (1) a low-density buffer layer of pyrolytic carbon ∿50 μm thick, (2) a high-density isotropic layer of pyrolytic carbon ∿35 μm, (3) a silicon carbide layer ∿30 μm thick, and (4) a second high-density isotropic pyrolytic carbon layer ∿35 μm thick.

Following coating, the particles pass to the Fuel Rod Fabrication step where they are blended with fertile ThO_2 coated particles and inert graphite shim and dispensed into molds. These are then injected with a matrix of heated pitch and graphite powder that fills the interstices between particles to form a solid fuel rod. A typical fuel rod is a right circular cylinder about 13 mm in diameter and 50 mm in length.

In the final process step, the rods are loaded into fuel blocks and carbonized in place by passing the blocks through a whole-block carbonization and annealing furnace. The finished product is cleaned and inspected before it is canned for shipping.

Throughout the process, samples will be extracted from the process line and diverted to Sample Inspection for quality control and assurance purposes. In addition, substantial quantities of reject material are anticipated from a number of process steps. This material, plus samples returned from the Sample Inspection Station, will be routed to Scrap and Waste for appropriate recycle and disposal. Figure 5 shows the fuel components at various stages of the process.

A more detailed description of the HTGR fuel refabrication process can be found in Ref. 21.

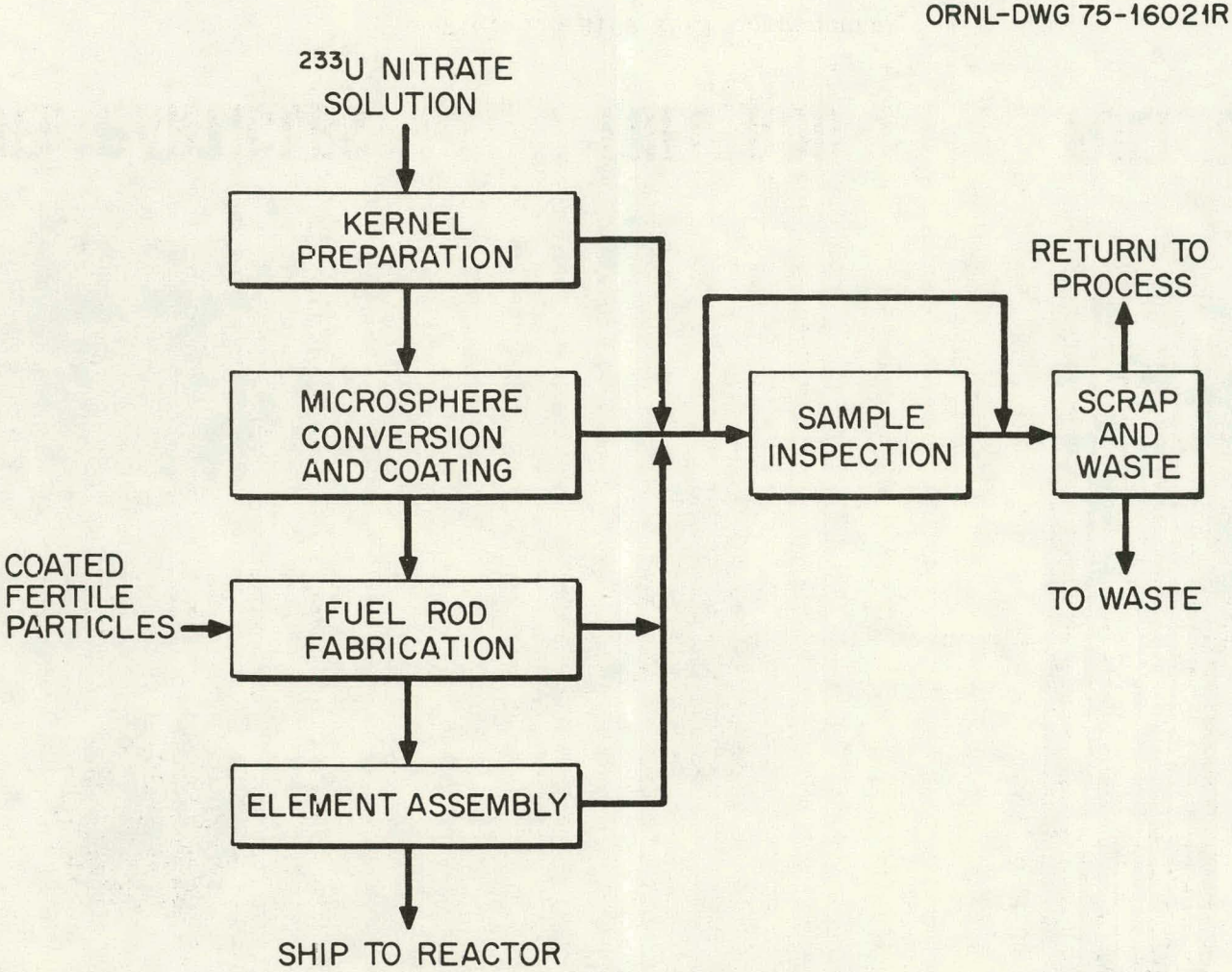

Fig. 4. Process for HTGR fuel refabrication.

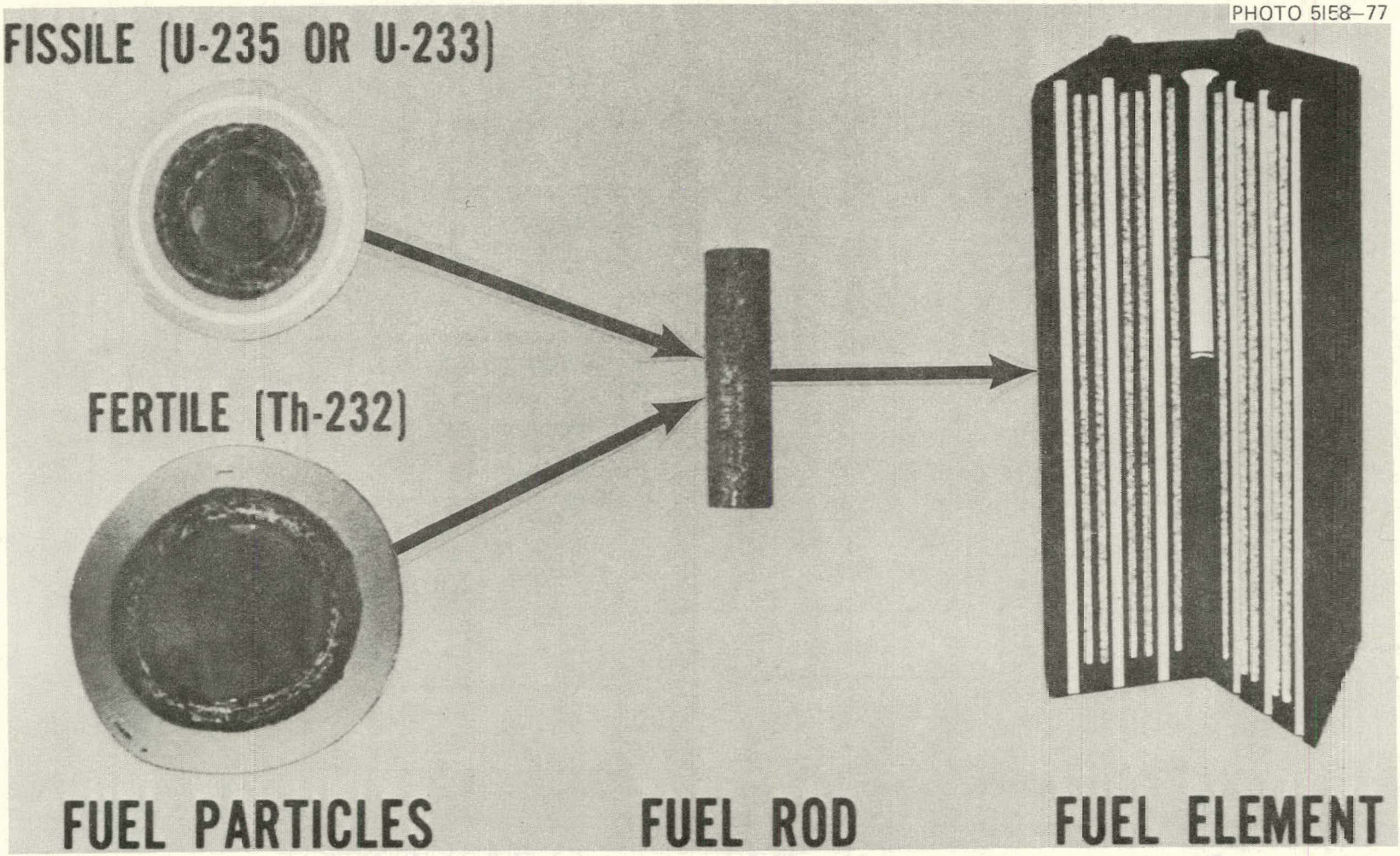

Fig. 5. HTGR fuel components.

3. FUEL PARTICLE STORAGE HOPPERS

As described in the previous section, ^{233}U will be found in several different material forms during the refabrication process. One form consists of ^{233}U microspheres that may be bare or coated with successive layers of carbon and silicon carbide. The design of storage hoppers to contain fuel particles in all stages of processing is restrained by criticality safety requirements.

A criticality analysis of the storage hoppers begins with a reference description of the fuel particles encountered in the refabrication process. Table 16 lists the physical properties of fuel particles and their coatings at various stages of production.

Table 16. Physical properties of HTGR fuel particles in various stages of refabrication

Particle type	Physical properties[a]
Dried uranium loaded resin	47 wt % ^{233}U in resin of $C_6O_2H_6$ Particle density = 1.7 gms/cm^3
Carbonized resin	73 wt % ^{233}U, 17 wt % C, 10 wt % O Particle density = 3.3 gms/cm^3
Converted kernel	$^{233}UC_3O_{0.5}$ Particle density = 3.2 gms/cm^3 Particle diameter = 400 microns
Buffer coated particle	Pure carbon coating Coating density = 1.1 gms/cm^3 Coating thickness = 50 microns
ILTI coated particle	Pure carbon coating Coating density = 1.85 gms/cm^3 Coating thickness = 35 microns
SiC coated particle	Pure SiC coating Coating density = 3.2 gms/cm^3 Coating thickness = 30 microns
OLTI coated particle	Pure carbon coating Coating density = 1.85 gms/cm^3 Coating thickness = 35 microns

[a]For conservatism, we have assumed that all uranium is ^{233}U.

The specification of a critically safe hopper for these fuel particles requires that the effective neutron multiplication factor, k_{eff}, of the hopper-particles-surroundings system be less than 1.0 by an amount known as the safety margin. The safety margin will be dependent upon the degree of uncertainty associated with (1) expected particle properties and packing fractions, (2) hopper surroundings, (3) criticality calculational ability, (4) experimental criticality data and (5) process accident conditions. Accidental operation conditions that must be considered include dimensional changes due to bulging and container breakage, operational errors such as double batching, water flooding and densification of fissile material, and changes in the system surroundings.

In general, safety criteria for problems of this type are obtained from guidelines found in criticality safety manuals. For example, ANSI N16.1-1975[1] lists the maximum subcritical diameter of 11.5 cm for a cylindrical vessel containing a ^{233}U water slurry under the most reactive conditions. Combining this restriction with the fact that water slurries of all the types of particles described in Table 16 are more reactive than a dry bed of particles leads to a conclusion that the 11.5 cm limit would provide a safe diameter for cylindrical hoppers.* However, this limit imposes significant economic penalties on a production facility. Relaxation of this limit would contribute to a more efficient operation. Hence, several calculations were performed to investigate the criticality aspects of larger diameter storage hoppers.

The following section describes hopper models that were calculated by the ANISN[17] computer code using Hansen-Roach[1] cross sections.

3.1 Criticality Calculations

3.1.1 Infinite cylinder models containing dry particles

For these cases, isolated storage hoppers were modeled as infinite cylinders consisting of an inner particle chamber surrounded by an outer

*This assumes that highly effective neutron reflectors such as beryllium and D_2O will not be present.

0.318 cm thick wall of stainless steel. The particle chambers were filled with each of the seven particle types (62% packing fraction).

Critical diameters for the chambers and effective multiplication constants for a 22.9-cm (9.0 in.) diameter chamber were calculated. The results are given in Table 17. It is important to note that these calculations are for dry particle beds.

Table 17. Results of criticality calculations on infinite cylinder models of particle storage hoppers

Particle type	k_{eff} 22.9-cm (9.0-in.) diameter particle chamber	Critical diameter (cm) of particle chamber
Dry loaded resin	0.396 0.884 (with additional H_2O reflector)	47.9 28.5 (with additional H_2 reflector)
Carbonized resin	0.339	64.0
Converted kernel	0.351	67.3
Buffer coated	0.200	92.3
ILTI	0.151	95.6
SiC coated	0.123	100.5
OLTI coated	0.095	105.8

To examine the effect of reflectors, one system (dry loaded resin, the most reactive) was calculated with an additional reflector of 20 cm of water placed around the stainless steel wall. It is observed that the water reflector significantly increased the system reactivity.

3.1.2 Water flooded-water reflected spherical model

A hopper design that will eliminate the possibility of accidental criticality solely on the basis of hopper geometry even when the hopper is water filled and reflected and the particles levitated to obtain an optimum $H/^{233}U$ ratio is desirable. If a spherical hopper can be designed to meet the above criteria, then an equal volume cylindrical hopper will also meet these requirements. To this end, we have estimated the critical

volumes for each particle type over the range of all possible water-particle mixtures.

The model consists of a spherical core containing a water-particle mixture surrounded by a thick water reflector. The minimum critical volumes were approximated through the use of calculations performed by Thomas[11] which are based upon ANISN calculations using Hansen-Roach cross sections. Although Thomas' results pertain to $^{233}UO_2$-C mixtures, they can be applied to our problem under the assumption that the controlling criticality parameters at high H/^{233}U ratio are the H/^{233}U ratio and the ^{233}U density. The results are given in Table 18.

Table 18. Estimated minimum critical volumes obtainable in water flooded — water reflected systems of HTGR fuel particles in various stages of refabrication

Particle type[a]	Estimated minimum critical volume[b] (liters)
Uranium loaded resin	5.7
Carbonized resin	4.8
Converted kernels	4.6
Buffer coated	5.6
ILTI coated	6.3
SiC coated	6.8
OLTI coated	8.2

[a] All uranium taken to be ^{233}U.

[b] Estimated accuracy is ±10%.

Particle storage hoppers with volumes smaller than those listed in the table will remain subcritical under all conditions of water flooding. We note that hoppers in the Microsphere Conversion and Coating system will likely be multi-purpose and consequently will be limited in volume by restrictions imposed on converted kernel material. It should also be pointed out that the volume limits could be increased by about a factor of two if the effects of a water reflector could be eliminated.

A coating of boron or cadmium on the outside of the hoppers could achieve this isolation.

3.2 Conclusions

1. Isolated fuel particle storage hoppers of cylindrical geometry will be critically safe under all conditions of water flooding and water reflection provided their diameter is less than 11.5 cm. This assumes that the cylindrical vessel limit for ^{233}U slurries as published in ANSI N16.1-1975[1] is a valid limit (see Sect. I-7).
2. Isolated hoppers 22.9-cm (9.0-in.) in diameter are critically safe for all particle types provided that no strong neutron moderators (such as water or other hydrogenous material) are present in the particle bed.
3. Careful design of hopper shapes, sizes and material construction could result in hoppers that are subcritical even when flooded and surrounded by a water reflector. These designs could include a neutron poison to decouple the fuel particle chamber from the reflector.

4. RESIN CARBONIZATION FURNACE

One process step in the refabrication of HTGR fuels consists of heat treating a fluidized bed of ^{233}U loaded resin particles to drive off the hydrogenous components and to form a $^{233}UO_2$-C particle. Factors affecting material processing and economics have indicated that a 22.9-cm (9.0-in.) diameter bed of fuel particles containing 3 kg of uranium would be desirable for this process. However, as in the case with particle storage hoppers, this system is a potential criticality hazard.

Figure 6 is a photograph of a proposed fluidized bed furnace showing the fluidizing chamber and the surrounding fire-brick insulation. Fluidizing gas enters the chamber through the central tube at the bottom and exhausts through the wrapped tube on top. After gas flow has been initiated, fuel particles can be introduced to the chamber via a port in the side. Upon completion of carbonization, the fluidizing gas is turned off and the carbonized particles exit the chamber through the gas inlet tube. A valve allows the particles to be transferred to a storage hopper.

As a first step in processing furnace off-gas, a perchloroethylene-based scrubber system receives all gases exiting from the furnace. Here particulate matter is removed from the off-gas by means of a series of spray nozzles mounted in a vertical column. The perchloroethylene spray collects in a reservoir at the bottom of the spray column before being pumped back through the nozzles. Fuel particles are occasionally carried over into the scrubber system where they settle to the bottom of the perchloroethylene reservoir.

Two problem areas can be identified as potentially dangerous (1) the fluidized bed chamber and (2) the reservoir region of the scrubber system. Each of these is examined in the following discussion.

Two fuel forms must be considered in a criticality analysis of this furnace system, the uncarbonized uranium loaded resin and its corresponding carbonized form. Table 16 in Sect. II-3 specifies the physical characteristics of the fuel particles. As in the case of the particle storage hoppers, the uncarbonized fuel particles are the most reactive material in a dry environment. This is primarily due to the presence of hydrogen in the resin. It must also be noted that uranium loaded resin

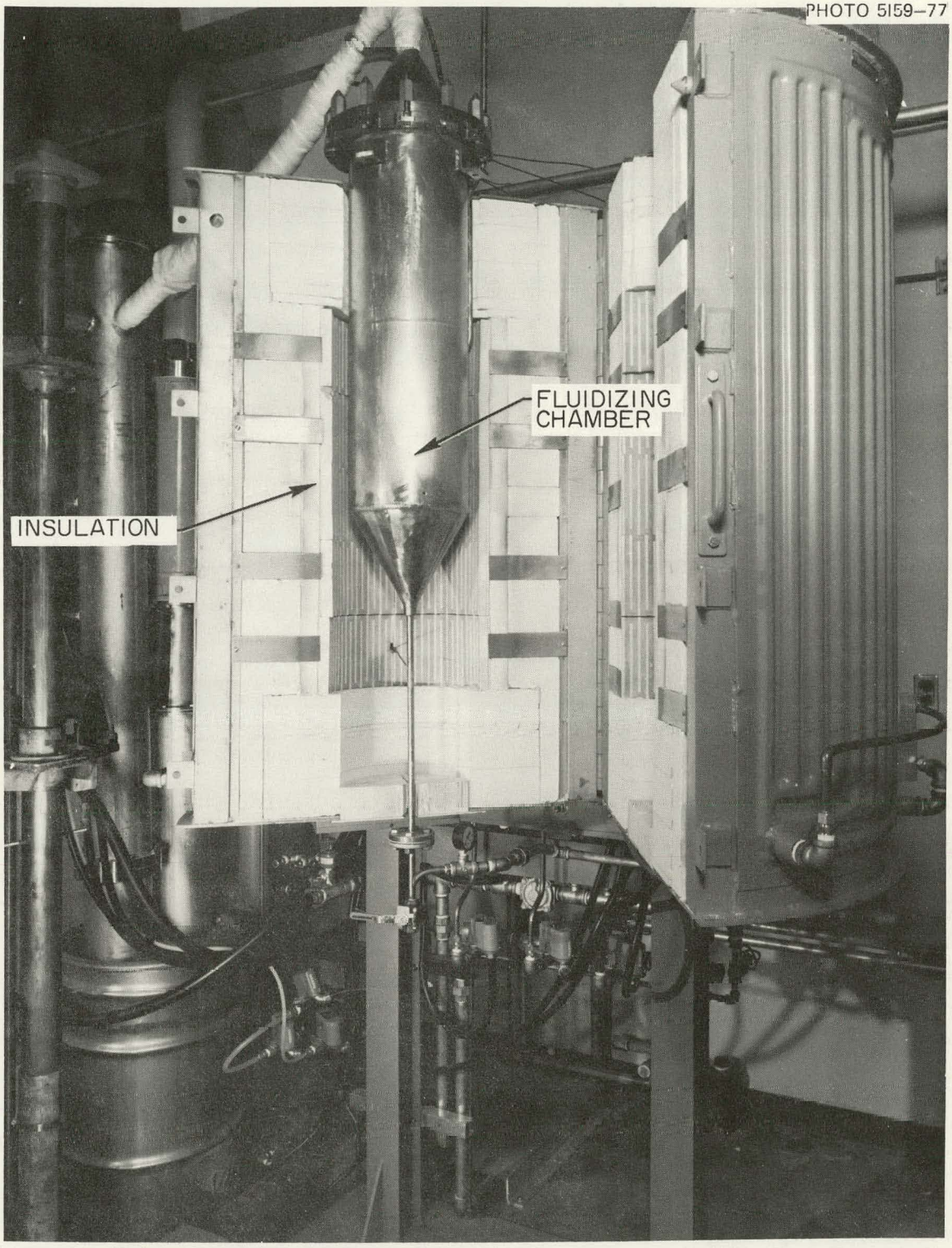

Fig. 6. HTGR fuel particle carbonization furnace.

could conceivably retain water from the loading process if an intermediate drying operation failed.

The following calculations were performed to determine the reactivity of fuel particles in the furnace environment.

4.1 Criticality Calculations

4.1.1 Infinite cylinder model of furnace

This model consists of an inner cylinder representing the fluidizing chamber surrounded by a thick annular region of insulating materials. For conservatism, the model is taken to be infinite in height. Variable parameters of interest are water content of uranium loaded resin, diameter of fluidizing chamber, and particle packing fraction in the bed. The uranium was taken to be 100% ^{233}U.

Figure 7 shows the results of calculations performed with ANISN and the 16-group Hansen-Roach cross section set. The weight percent H_2O in the loaded resin particle is limited to 30%, the saturation limit of the material. Particle packing fractions of 62% and 100% correspond to a packed bed of perfectly spherical particles and the limiting case of a conglomerated mass. From the figure we observe that the system reactivity is highly sensitive to the water content of the resin, the diameter of the fluidizing chamber and the packed particle density. Thus, these parameters must be closely controlled in a large furnace.

4.1.2 Finite cylinder model of furnace

To generate a closer approximation of the physical furnace system, a second cylindrical model was constructed with a finite height.* The model is essentially the same as the one described above with the exception that the height was restricted to that required to hold a packed bed of particles of a specified uranium content. In addition, rather than explicitly modeling the furnace walls in the regions above and below the particle bed, we approximated the effect of the walls by including a

*This model is still conservative with respect to geometry since the actual furnace will contain a conical section as the lower portion of the fluidizing chamber.

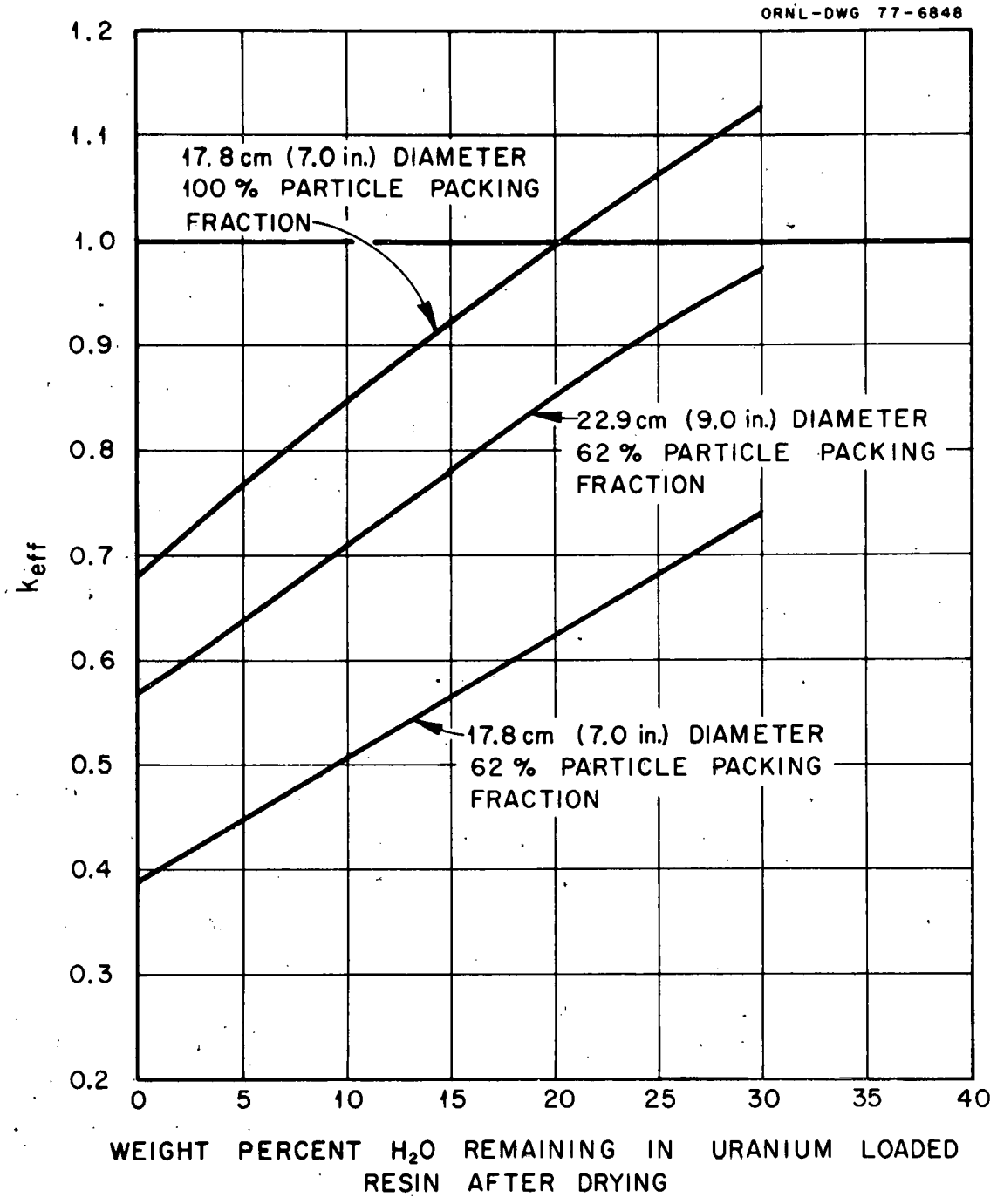

Fig. 7. Calculated k_{eff} for infinite cylinder model of resin carbonization furnace with different sized fluidizing chambers and different particle packing fractions.

5.08 cm (2.0 in.) thick reflector of fire brick on the top and bottom surface of the particle bed.

Using the KENO IV computer code, calculations were performed on several proposed systems with both the Hansen-Roach cross section set and the 123-group ENDF library described in Sect. I-4. Each calculated system had several features in common:

1. The fluidizing chamber contained two large batches of fuel particles having a total uranium mass of 7.0 kg (double batch).
2. Fuel particles were in the form of ^{233}U loaded resin with 30 weight percent retained water in the resin particle.
3. The wet resin particle density was taken as 1.88 gms/cm^3 with uranium forming 32.9 weight percent.
4. Fuel particles were close-packed with a 62 volume percent packing fraction.

Variable parameters investigated in the calculations were the diameter of the fluidizing chamber, and the content of the interstitual spaces in the particle bed. Table 19 presents the results of the calculations.

From the table we observe a severe reactivity increase due to flooding the packed bed with water. This illustrates the importance of excluding water from the particle bed of a large diameter furnace. It is interesting to note that flooding with pure perchloroethylene (C_2Cl_4) has a poisoning effect on the system reactivity. This can be explained by the neutron capture properties of the chlorine component. Also note that there exists a 7—9% calculational uncertainty due to uncertainty in selection of the "correct" cross section set.

These calculations only show the sensitivity of k_{eff} to the specified parameter changes; they do not give k_{eff} for the worst possible criticality condition. In addition the calculations were performed to provide general guidance for conceptual design decisions and as such do not necessarily represent situations that will be encountered in an operating facility. For instance, the assumption of a double-batch size of 7.0 kg of uranium may be realistic of a 22.9-cm furnace, but it is excessively large for a smaller furnace.

Table 19. Results of Monte Carlo calculations performed on finite height model of resin carbonization furnace

Model variables			Calculated k_{eff}	
Fluidizing chamber diameter (cm)	(in.)	Interstices	Hansen-Roach cross sections	ENDF/B-IV cross sections
17.8	7.0	Void	0.643 ± 0.005	—
17.8	7.0	H_2O	1.030 ± 0.007	1.120 ± 0.007
17.8	7.0	C_2Cl_4	0.583 ± 0.005	—
17.8	7.0	90% C_2Cl_4 10% kerosene[a]	0.637 ± 0.004	—
22.9	9.0	Void	0.785 ± 0.007	0.857 ± 0.005
22.9	9.0	H_2O	1.176 ± 0.006	1.261 ± 0.007
12.7	5.0	Void	0.437 ± 0.005	—
12.7	5.0	H_2O	0.772 ± 0.006	—

[a]Kerosene composition was taken to be 13.2 wt % hydrogen and 86.8 wt % carbon with a density of 0.845 gm/cm^3. This is equivalent to 13,200 wt ppm hydrogen in the mixture.

4.1.3 Spherical model of furnace off-gas scrubber reservoir

As stated in Sect. II-4 above, occasionally a fraction of the fuel particles will be carried out of the fluidizing chamber by the off-gas stream and enter an off-gas scrubber reservoir adjacent to the furnace. Accumulation of these particles in a perchloroethylene reservoir at the bottom of the scrubber has been examined for criticality safety.

To calculate this situation we defined a spherical model consisting of a mixture of uranium loaded resin particles and perchloroethylene. Two distributions of particles in the mixture were considered — a homogeneous distribution and one in which the particles were tightly packed in a central core surrounded by and saturated with perchloroethylene. In each case the outside diameter of the sphere was 55.9 cm (22.0 in.) and 4.0 kg of ^{233}U in the form of wet resin was contained within.

Table 20 gives the results of calculations obtained with ANISN and the 16-group Hansen-Roach cross section set. We see that the more reactive configuration contains the particles in a tightly packed wad, but both cases have low enough reactivity that particles in the scrubber do not appear to be a major problem provided that no more than a single charge of uranium particles are allowed to accumulate in the reservoir.

Table 20. Results of criticality calculations performed on spherical model of resin carbonization scrubber system

Model geometry	Calculated k_{eff}	
	Interstitial pure perchloroethylene	Interstitial perchloroethylene with 10% kerosene[a]
Particles tightly packed (62 vol %) into a sphere surrounded by and saturated with perchloroethylene	0.624	0.721
Particles uniformly distributed through the perchloroethylene	0.051	0.159

[a]Kerosene composition was taken to be 13.2 wt % hydrogen and 86.8 wt % carbon with a density of 0.845 gms/cm^3. This is equivalent to 13,200 wt ppm hydrogen in the mixture.

4.2 Conclusions

We draw the following conclusions concerning the criticality safety of the resin carbonization furnace-scrubber system.

1. It is possible to design a critically safe resin carbonization furnace having a fluidizing chamber approximately 22.9 cm (9.0 in.) in diameter provided that accidental flooding of the fluidizing chamber with a hydrogenous substance is impossible.
2. If flooding is not an impossibility, even a 17.8 cm (7.0 in.) diameter fluidizing chamber can go critical under certain conditions.
3. Criticality in the perchloroethylene reservoir of the off-gas scrubber because of the accumulation of "blown-over" particles does not appear to be a problem provided that the uranium mass in the reservoir does not exceed 4.0 kg and that hydrogenous materials do not constitute a large percentage of the scrubber solution.

ACKNOWLEDGMENT

The authors wish to thank the members of the Fuel Cycle Technology group of the Metals and Ceramics Division who supplied the information on the HTGR fuel refabrication process and fuel material properties. We are grateful to J. C. Cleveland for his critical review of this report. Thanks also to A. G. Mason who assisted in the performance of the calculations.

REFERENCES

1. *American National Standard for Nuclear Criticality Safety in Operations with Fissionable Materials Outside Reactors,* ANSI N16.1-1975, American National Standards Institute (April 1975).

2. H. C. Paxton, *Los Alamos Critical-Mass Data,* LA-3067-MS, Rev., Los Alamos Scientific Laboratory, p. 50 (December 1975).

3. J. K. Fox, L. W. Gilley, and E. R. Rohrer, *Critical Mass Studies, Part VIII, Aqueous Solutions of* ^{233}U, ORNL-2143 (September 1959).

4. J. T. Thomas, "Critical Experiments with Aqueous Solutions of $^{233}UO_2(NO_3)_2$," *Neutron Physics Division Annu. Progr. Rep. May 31, 1968,* ORNL-4280, pp. 53–55.

5. J. G. Bruna et al., "Resultats D'Experiences Critiques Homogenes Realisees Avec Le Plutonium-239, L'Uranium-235, et L'Uranium-233," *Criticality Control of Fissile Materials,* IAEA (1966).

6. J. T. Thomas, J. K. Fox and D. Callihan, "A Direct Comparison of Some Nuclear Properties of ^{233}U and ^{235}U," *Nucl. Sci. Eng.* 1, 20–32 (1956).

7. R. Gwin and D. W. Magnuson, "The Measurement of Eta and Other Nuclear Properties of ^{233}U and ^{235}U in Critical Aqueous Solutions," *Nucl. Sci. Eng.* 12, 364–380 (1962).

8. J. K. Fox et al., "Critical Parameters of Uranium Solutions in Simple Geometry," *Neutron Physics Division Annu. Progr. Rep. Sept. 1, 1958,* ORNL-2609, p. 42.

9. J. Wallace Webster, *Calculated Neutron Multiplication Factors of Uniform Aqueous Solutions of* ^{233}U *and* ^{235}U, ORNL-CDC-2 (October 1967).

10. S. R. Bierman and E. D. Clayton, *High Temperature Gas-Cooled Reactor Criticality Research Program,* BNWL-2115 (June 1976).

11. J. T. Thomas, *Calculated Criticality of Water Moderated Oxides of Uranium-233, Thorium-232, and Carbon Mixtures,* Y-DR-107, Union Carbide Corporation, Y-12 Plant (1973).

12. G. E. Hansen and W. H. Roach, *Six and Sixteen Group Cross Sections for Fast and Intermediate Critical Assemblies,* LAMS-2543, Los Alamos Scientific Laboratory (1961).

13. S. R. Biermann and E. D. Clayton, *Status of HTGR Criticality Safety Data Needs on U-Th Fuel Cycle,* Research Report, Battelle Pacific Northwest Laboratories (June 1975).

14. M. K. Drake (Ed.), *Data Formats and Procedures for the ENDF Neutron Cross Section Library,* BNL-50274 (T-601), Brookhaven National Laboratory (October 1970).

15. N. M. Greene et al., *AMPX: A Modular Code System for Generating Coupled Multigroup Neutron-Gamma Libraries from ENDF/B,* ORNL/TM-3706 (March 1976).

16. L. W. Nordheim, "The Theory of Resonance Absorption," *Proc. of Symposia in Applied Mathematics*, Garret Birkhoff and E. P. Wigner, Eds., Vol. XI, p. 58, American Mathematical Society (1961).

17. W. W. Engle, Jr., *A Users Manual for ANISN: A One-Dimensional Discrete Ordinates Transport Code with Anisotropic Scattering*, K-1693, Union Carbide Gaseous Diffusion Plant (1967).

18. L. M. Petrie and N. F. Cross, *KENO IV: An Improved Monte Carlo Criticality Program*, ORNL-4938 (November 1975).

19. N. M. Steen, *Analysis of the Fission Neutron Spectrum of ^{233}U and Criticality Computations for Homogeneous $^{233}U - H_2O$ Spheres and Cylinders*, WAPD-TM-997 (June 1972).

20. J. K. Fox et al., "Critical Parameters of Aqueous Solutions of ^{235}U," *Applied Nuclear Physics Progr. Rep. Sept. 1, 1957*, ORNL-2389, pp. 71–83.

21. J. D. Sease and A. L. Lotts, *Development of Processes and Equipment for the Refabrication of HTGR Fuels*, ORNL/TM-5334 (June 1976).

ORNL/TM-6136
Dist. Category UC-77

Internal Distribution

1. E. J. Allen
2. P. Angelini
3. S. Baron
4. B. J. Baxter
5. R. J. Beaver
6. E. D. Blakeman
7. R. A. Bradley
8. A. J. Caputo
9. J. A. Carpenter
10. W. L. Carter
11. J. C. Cleveland
12. D. A. Costanzo
13. F. C. Davis
14. R. G. Donnelly
15. J. P. Drago
16. W. P. Eatherly
17. J. R. Engel
18. J. I. Federer
19. D. E. Ferguson
20. A. J. Frankel
21. N. M. Greene
22. P. A. Haas
23. J. F. Harvey
24. C. C. Haws
25. R. E. Helms
26. L. C. Hensley
27. M. R. Hill
28. F. J. Homan
29–38. J. D. Jenkins
39. D. R. Johnson
40. M. J. Kania
41. P. R. Kasten
42. H. T. Kerr
43. W. J. Lackey
44. M. Levenson
45. A. L. Lotts
46. A. P. Malinauskas
47. J. E. Mack
48. M. M. Martin
49–58. S. R. McNeany
59. J. T. Mihalczo
60. K. J. Notz
61. A. R. Olsen
62. A. E. Pasto
63. L. M. Petrie
64. H. Postma
65. D. P. Reid
66. D. J. Richards
67. J. M. Robbins
68. J. E. Rushton
69. T. F. Scanlan
70. C. D. Scott
71. J. E. Selle
72. J. H. Shaffer
73. M. R. Sheldon
74. I. Spiewak
75. D. P. Stinton
76. R. R. Suchomel
77. V. J. Tennery
78. J. T. Thomas
79. S. J. Tiegs
80. T. N. Tiegs
81. H. E. Trammell
82. D. B. Trauger
83. J. R. Weir, Jr.
84. R. M. Westfall
85. G. E. Whitesides
86. R. G. Wymer
87. R. M. Young
88–89. Central Research Library
90. Document Reference Section
91–92. Laboratory Records Department
93. Laboratory Records, ORNL RC
94. ORNL Patent Office

External Distribution

95–96. Director, Office of Fuel Cycle Evaluation, DOE, Washington, DC 20545

97–98. Director, Division of Nuclear Fuel Cycle and Production, DOE, Washington, DC 20545

99. R. G. Bradley, Division of Nuclear Fuel Cycle and Production, DOE, Washington, DC 20545

100–104. W. S. Schieb, Division of Nuclear Fuel Cycle and Production, DOE, Washington, DC 20545
105. C. E. Williams, Manager, DOE Idaho Operations Office, P.O. Box 2108, Idaho Falls, ID 83401
106. Barry Smith, DOE Idaho Operations Office, P.O. Box 2108, Idaho Falls, ID 83401
107. J. B. Radcliffe, DOE Office of Program Management, Research and Space Programs, P.O. Box 81325, San Diego, CA 92138
108. R. D. Thorne, Manager, DOE San Francisco Operations Office, 1333 Broadway, Wells Fargo Bldg., Oakland, CA 94612
109. Director, Reactor Division, DOE, ORO
110. Director, Research and Technical Support Division, DOE, ORO
111. F. E. Dearing, Reactor Division, DOE, ORO
112–288. For distribution as shown in TID-4500 under UC-77, Gas Cooled Reactor Technology.